Robotica (2014) volume 32, pp. 783–802. © Cambridge University Press 2013
doi:10.1017/S0263574713001069

Adaptive manipulation and slippage control of an object in a multi-robot cooperative system

Shahram Hadian Jazi†,*, Mehdi Keshmiri§, Farid Sheikholeslam¶, Mostafa Ghobadi Shahreza§ and Mohammad Keshmiri††

†*Engineering Department, University of Isfahan, Isfahan, Iran*
§*Department of Mechanical Engineering, Isfahan University of Technology, Isfahan, Iran*
¶*Department of Electrical and Computer Engineering, Isfahan University of Technology, Isfahan, Iran*
†† *Mechanical and Industrial Engineering, Concordia University, Montreal, Canada*

(Accepted October 29, 2013. First published online: December 3, 2013)

SUMMARY
Considering undesired slippage between manipulated object and finger tips of a multi-robot system, adaptive control synthesis of the object grasping and manipulation is addressed in this paper. Although many studies can be found in the literature dealing with grasp analysis and grasp synthesis, most assume no slippage between the finger tips and the object. Slippage can occur for many reasons such as disturbances, uncertainties in parameters, and dynamics of the system. In this paper, system dynamics is analyzed using a new presentation of friction and slippage dynamics. Then an adaptive control law is proposed for trajectory tracking and slippage control of the object as well as compensation for parameter uncertainties of the system, such as mass properties and coefficients of friction. Stability of the proposed adaptive controller is studied analytically and the performance of the system is studied numerically.

KEYWORDS: Adaptive control; Slippage control; Cooperative robots; Frictional contacts.

Nomenclature

$\mathbf{B}$	Coefficient matrix of the input torques
$\tilde{\mathbf{B}}$	Coefficient matrix of the input torques in reduced order form
${}_{\mathrm{I}}\mathbf{C}_{\mathrm{o}}$	Rotation matrix of the object frame with respect to the inertial frame
${}_{\mathrm{I}}\mathbf{C}_{\mathrm{c_i}}$	Rotation matrix of the *i*th contact frame with respect to the inertial frame
$\mathbf{F}$	Vector consisting of friction and normal forces exerted by end-effector on the object
$\mathbf{h}$	Coriolis-centrifugal-gravity matrix
$\tilde{\mathbf{h}}$	Coriolis-centrifugal-gravity matrix in reduced order form
$\mathbf{I}$	Identity matrix
I_{o}	Object moment of inertia
$\mathbf{J}$	Jacobian matrix
$\mathbf{K}_p$	Constant semi-positive definite matrix
$\mathbf{K}_v$	Constant positive definite matrix
k	Number of joints
l	Length of manipulator's link
L_{o}	Distance between the object center of mass and its edges

* Corresponding author. E-mail: s.hadian@eng.ui.ac.ir

$\mathbf{M}$	Inertia matrix
$\tilde{\mathbf{M}}$	Inertia matrix in reduced order form
m	Mass of manipulator's link
m_{o}	Object mass
n	Number of manipulators
$\boldsymbol{p}$	Description of $\vec{\mathbf{r}}_{\mathbf{c}}$ in the object frame
$\mathbf{q}$	Vector of generalized coordinates
q	Generalized coordinate of manipulator's joint
$\vec{\mathbf{R}}_{\mathrm{e}}$	Vectorial form of position vector of end-effector with respect to the inertial frame
$\vec{\mathbf{R}}_{\mathrm{o}}$	Vectorial form of position vector of the object center of mass with respect to the inertial frame
$\mathbf{R}_{\mathrm{e}}$	Column vector description of $\vec{\mathbf{R}}_{\mathrm{e}}$
$\mathbf{R}_{\mathrm{o}}$	Column vector description of $\vec{\mathbf{R}}_{\mathrm{o}}$
$\vec{\mathbf{r}}_{\mathbf{c}}$	Position vector of the adjacent point on the object and end-effector at the contact point
$\mathbf{s}$	Vector of slippage states
s	Slippage state
s_x	Slippage state in x direction
s_y	Slippage state in y direction
$\mathbf{U}$	Regression matrix
V	Lyapunov function
$\mathbf{W}$	Grasping matrix
$\mathbf{x}$	Vector of output coordinates
$x_{\mathrm{o}}^{\mathrm{des}}(t)$	Desired trajectory of the object in x direction
$y_{\mathrm{o}}^{\mathrm{des}}(t)$	Desired trajectory of the object in y direction
θ_{o}	Vector of the generalized coordinates representing the object orientation
$\theta_{\mathrm{o}}^{\mathrm{des}}(t)$	Desired trajectory of the object orientation
$\boldsymbol{\Gamma}$	Constant positive definite matrix
μ	Coefficient of friction
τ	Generalized driving force/torque
$\boldsymbol{\varphi}$	Vector of unknown parameters
φ_0	Upper bound for norm of the unknown parameters vector
$(\hat{\bullet})$	Estimated value
$(\bullet)_{\mathrm{i}}$	ith manipulator parameter and variable
$(\bullet)_{\mathrm{o}}$	Object parameter and variable
$(\bar{\bullet})$	Actual value

1. Introduction

Object grasping and manipulation, especially in multi-arm systems, multi-fingered hands, or multi-agent robotic systems, have received considerable attention over the past few years. A large number of them have focused on system dynamics and control.

Many types of robotic hands and grippers are designed and constructed to perform a stable grasping and manipulation. Stable grasp is suggestive of appropriate forces and desired constraints imposed on the object for the external forces exerted and disturbances caused. These forces and constraints must satisfy the equilibrium and friction conditions, the constraints imposed by the system, as well as the conditions corresponding to the inward normal contact forces.

The most related topics in the field of object grasping can be categorized into two fundamental classes: grasp analysis and grasp synthesis. In fact the form/force closure is the main target in grasping, finding appropriate conditions for form/force closure grasp is the main focus in grasp analysis, while finding optimality criteria and developing proper algorithms for computing the contact locations is the core of grasp synthesis.

Early works in grasp analysis are done by Reulaux[1] in 1963, and Salisbury and Roth[2] in 1983. They introduced the concept of force/form closure and several contact types. Mishra *et al.*[3] in 1987 studied positive grips and introduced the bounds of the number of fingers for gripping an object for different load conditions. They also introduced an algorithm to find the number of fingers needed

https://doi.org/10.1017/S0263574713001069 Published online by Cambridge University Press

to grip polygonal/polyhedral objects. Bicchi[4] in 1995 handled form and force closure properties and partial form and force closure. He also introduced an algorithm to synthesize partial form-closure properties. He proved that force-closure analysis is equal to the equilibrium of an ordinary differential equation.

Bounab *et al*.[5] in 2008 proposed new conditions for an *n*-hard finger hand to obtain force-closure grasp, using the central axes of the grasp wrench. Kruger *et al*.[6] in 2011 extended and defined the conditions for partial force-closure grasps. They used the maximum and the sum of the contact forces to achieve the task wrench required for the grasped object.

In grasp synthesis, Mishra *et al*.,[3] Park and Starr,[7] Tung and Kak,[8] Cheong *et al*.,[9] Al-Gallaf,[10] Xue *et al*.,[11] Krug *et al*.,[12] and many other researchers[13–18] introduced a variety of optimality criteria and efficient algorithms for different multi-fingered robotic applications and types of manipulated object. The common assumption in the above studies is to consider the fixed contact between the finger tip and the manipulated object during cooperating manipulation.

Concerning sliding contacts, Kao and Cutkosky[19] in 1993 compared the theoretical and experimental sliding motions for a sheet of paper or a similar object on a planar surface with a two-fingered hand using the static equilibrium equations. Chong *et al*.[20] in 1993 proposed a motion/force planning algorithm for multi-fingered hands manipulating an object of an arbitrary shape using both rolling and sliding contacts. They used a nonlinear optimization approach to calculate the joint velocities and contact forces at each time step. Cole *et al*.[21] in 1992 considered control of the sliding motion of the fingertip of a two-fingered hand along the object surface as well as the position and orientation control of the object. They assumed that only one specific finger slides on a predefined path on the object surface. Their work is used to regrasp an object held in one hand. Zheng *et al*.[22] in 2000 addressed dynamic analysis and control synthesis of a three-fingered hand manipulating and regrasping an object in a three-dimensional space. They allowed one finger to slide on a predefined path on the object surface in order to change the grasp location. Phoka and Sudsang[23] in 2010 introduced a method for finger repositioning on the surface of a polygon to ensure force-closure grasp during object manipulation. In a finger-repositioning approach, they considered sliding or rolling the finger tip on the object surface.

Although the above studies considered the slippage in object regrasping analysis, the slippage should be completely predefined according to their methods. The fingers sliding on the object surface, the starting time, and duration of slippage as well as the sliding path should be known in advance. This means that the dynamic analysis and control synthesis of the undesired slippage continues to be undiscussed in the literature. But it can occur during the grasping maneuver due to parameter uncertainties, changing object geometry, mass, inertia, and coefficients of friction between the finger tips and the object.

To solve this problem, the authors of this paper began to study the undesired slippage dynamics and control. Dynamics analysis and control synthesis of the undesired slippage of a one-fingered hand pushing an object on the floor was initially discussed.[24] In this work, introducing a new model of frictional contacts, a multi-phases controller was designed to control the object motion and undesired slippage on the finger tip of the robot manipulator. The stability of the controller was proved analytically and the performance studied both numerically and experimentally. Figure 1 shows the experimental setup used. The setup consists of a two-link manipulator, a slider block, a slider railway, a control board, and a longitudinal motion measurement encoder. The control board box itself contains all the electronic hardwares: a 16-axis motion controller out of which only three of them are used, three amplifiers, the PCB interface board, and the corresponding wiring.

Continuing this study, the problem of undesired finger tip slippage control in a multi-fingered object manipulating system was addressed in ref. [25]. The present work is an extension of the previous works, concerning a multi-fingered hand manipulation with such parameter uncertainties in the system as mass properties and friction coefficients. As it is mentioned, in ref. [24] slippage control in a single robot manipulation is studied while in ref. [25] the approach has been extended to cooperating manipulations. In these two works, it is assumed that there is no uncertainty in the modeling. The current work extends ref. [25] to cooperating systems with uncertainties and deals with these uncertainties through an adaptive control approach.

The paper is organized in eight sections. In Section 2, for the slippage on the finger tips, a new dynamic analysis of a multi-fingered hand manipulating an object with frictional point contacts is addressed. This study is based on a new modeling of frictional conditions. Then, in Section 3,

https://doi.org/10.1017/S0263574713001069 Published online by Cambridge University Press

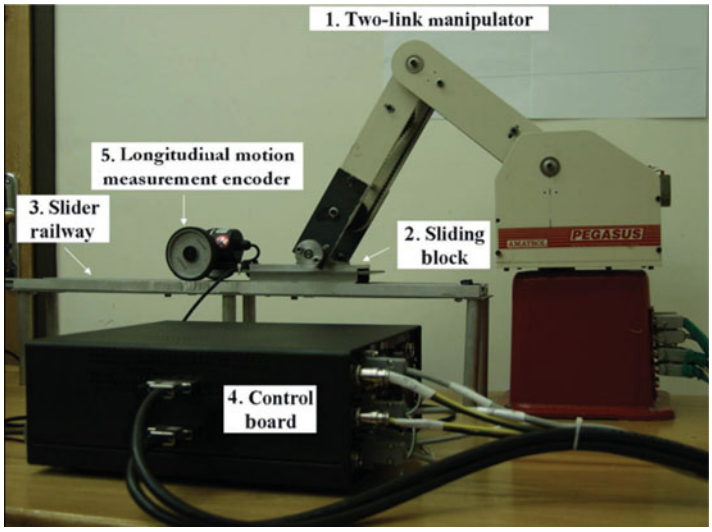

Fig. 1. (Colour online) Experimental setup used in authors' previous work.

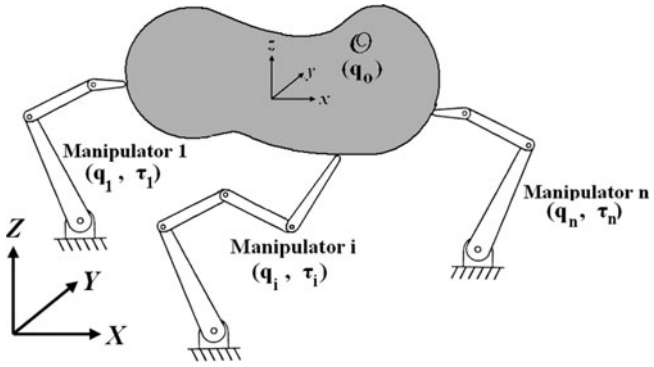

Fig. 2. Schematic of a multi-fingered hand manipulating an object.

adaptive controller and its update rule is proposed such that slippage error and its velocity as well as estimation for unknown parameters remain bounded. In Section 4, a two-fingered hand is introduced as a sample case and the motion equations are derived. Numerical results are also provided in this section. Section 5 provides conclusions.

2. Dynamic Analysis

Let us consider a multi-fingered hand system consisting of n fingers manipulating an object, O. The system is shown in Fig. 2. Each finger is a serial manipulator with k_i $(i = 1, 2, .., n)$ links.

The contact between each finger and the object is assumed to be the frictional point contact that can be moved along the object surface, but it is fixed on the tip of the finger. Note that without the last assumption, an additional kinematics problem must also be considered.

Due to constrained motion, the dynamic equations of the motion of each manipulator can be written as

$$\mathbf{M}_i\ddot{\mathbf{q}}_i + \mathbf{h}_i = \mathbf{B}_i\tau_i - \mathbf{J}_i^{\mathrm{T}}\mathbf{F}_i \quad (\mathrm{i} = 1,2,\ldots,\mathrm{n}), \tag{1}$$

where $\mathbf{q}_i$ and τ_i are the generalized coordinates and driving force/torque, respectively. $\mathbf{M}_i$ is inertia matrix, $\mathbf{h}_i$ is the coriolis-centrifugal-gravity term, $\mathbf{J}_i$ is Jacobian matrix of the ith finger, and $\mathbf{B}_i$ is the coefficient matrix of the input torques. $\mathbf{F}_i$ is a vector consisting of friction and normal forces exerted

https://doi.org/10.1017/S0263574713001069 Published online by Cambridge University Press

Table I. Values for α, β, and γ in different conditions.

	$\dot{s}$					
		$\dot{s}=0$				
	$\dot{s}\neq 0$	$\ddot{s}^{-}\neq 0$		$\ddot{s}^{-}=0$		
	Movement	Motion reversing	No motion	No motion	Start forward	Start backward
α	0	0	1	1	0	0
β	1	1	0	0	1	1
γ	Sign($\dot{s}$)	0	0	0	1	–1

by the *i*th end-effector on the object,

$$\mathbf{F}_{\mathrm{i}} = [F_{xi}, F_{yi}, F_{ni}]^T \quad (\mathrm{i} = 1,2,\ldots,\mathrm{n}). \tag{2}$$

where F_{xi}, F_{yi}, and F_{ni}, are the *i*th contact force components in the local contact frame, i.e., the *xy* contact surface and *n* normal direction to the contact surface. Note that since $\mathbf{F}_{\mathrm{i}}$ is defined as the vector of tangential and normal forces, the corresponding rotation matrix is included in $\mathbf{J}_{\mathrm{i}}$ matrix.

The object equations of motion are simply given by

$$\mathbf{M}_{\mathrm{o}}\ddot{\mathbf{q}}_{\mathrm{o}} + \mathbf{h}_{\mathrm{o}} = \sum_{\mathrm{i}=1}^{\mathrm{n}} \mathbf{W}_{\mathrm{i}}\mathbf{F}_{\mathrm{i}} = \mathbf{W}\mathbf{F}, \tag{3}$$

where $\mathbf{q}_{\mathrm{o}}$ is the set of generalized coordinates contributed by the object, $\mathbf{W}$ is the grasping matrix that can be written as

$$\mathbf{W} = \begin{bmatrix} \mathbf{W}_1 & \ldots & \mathbf{W}_{\mathrm{n}} \end{bmatrix}, \tag{4}$$

and

$$\mathbf{F} = \begin{bmatrix} \mathbf{F}_1^{\mathrm{T}} & \ldots & \mathbf{F}_{\mathrm{n}}^{\mathrm{T}} \end{bmatrix}^{\mathrm{T}}. \tag{5}$$

Where $\mathbf{W}_{\mathrm{i}}$ is grasping matrix due to i-th contact point.

For three-dimensional cases, two slippage states are needed to describe the slippage of each end-effector on the object, for example, s_{xi} and s_{yi}. Using these states, the new second-order equation with switching parameters for the frictional point contact presented in ref. [24] is used for modeling the contact force and motion conditions,

$$\alpha_{xi}\ddot{s}_{xi} + \begin{bmatrix} \beta_{xi} & \gamma_{xi}\mu_{xi} \end{bmatrix} \begin{Bmatrix} F_{xi} \\ F_{ni} \end{Bmatrix} = 0, \quad \alpha_{yi}\ddot{s}_{yi} + \begin{bmatrix} \beta_{yi} & \gamma_{yi}\mu_{yi} \end{bmatrix} \begin{Bmatrix} F_{yi} \\ F_{ni} \end{Bmatrix} = 0 \quad (i = 1, 2, \ldots n). \tag{6}$$

The above equations can be written in the following matrix form

$$\begin{bmatrix} \alpha_{xi} & 0 \\ 0 & \alpha_{yi} \end{bmatrix} \begin{Bmatrix} \ddot{s}_{xi} \\ \ddot{s}_{yi} \end{Bmatrix} + \begin{bmatrix} \beta_{xi} & 0 & \gamma_{xi}\mu_{xi} \\ 0 & \beta_{yi} & \gamma_{yi}\mu_{yi} \end{bmatrix} \begin{Bmatrix} F_{xi} \\ F_{yi} \\ F_{ni} \end{Bmatrix} = 0 \quad (i = 1, 2, \ldots n), \tag{7}$$

α, β, and γ coefficients in each direction are evaluated from Table I. More details of these formulation and coefficients can be found in refs. [24] and [25].

With some proper matrix definitions, the above equation is transformed into the following equation,

$$\boldsymbol{\alpha}_i\ddot{\mathbf{s}}_i + \mathbf{D}_i\mathbf{F}_i = 0 \quad (i = 1, 2, \ldots n), \tag{8}$$

https://doi.org/10.1017/S0263574713001069 Published online by Cambridge University Press

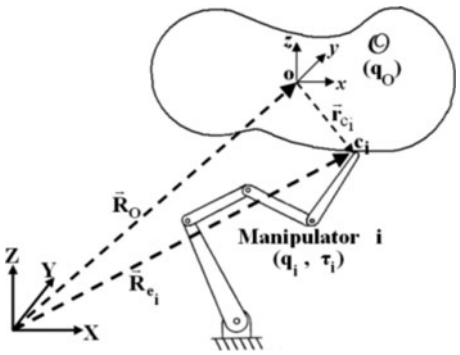

Fig. 3. Kinematics constraint in *i*th contact.

where

$$\boldsymbol{\alpha}_i = \begin{bmatrix} \alpha_{xi} & 0 \\ 0 & \alpha_{yi} \end{bmatrix}, \quad \mathbf{s}_i = \begin{Bmatrix} \ddot{s}_{xi} \\ \ddot{s}_{yi} \end{Bmatrix}, \quad \mathbf{D}_i = \begin{bmatrix} \beta_{xi} & 0 & \gamma_{xi}\mu_{xi} \\ 0 & \beta_{yi} & \gamma_{yi}\mu_{yi} \end{bmatrix}, \quad \mathbf{F}_i = \begin{Bmatrix} F_{xi} \\ F_{yi} \\ F_{ni} \end{Bmatrix}. \tag{9}$$

For *n* contact points, one can assemble the above equation as follows,

$$\boldsymbol{\alpha}_{|2n\times 2n}\, \ddot{\mathbf{s}}_{|2n\times 1} + \mathbf{D}_{|2n\times 3n}\, \mathbf{F}_{|3n\times 1} = \mathbf{0}. \tag{10}$$

Since the system under consideration is kinematically constrained, kinematics constraint equations should be added to the above equations of motion. For each contact point the kinematics constraint can be written as

$$\vec{\mathbf{R}}_{e_i} = \vec{\mathbf{R}}_o + \vec{\mathbf{r}}_{c_i}, \quad i = 1, \ldots, n. \tag{11}$$

As shown in Fig. 3, $\vec{\mathbf{R}}_o$ is the position vector of the object center of mass and $\vec{\mathbf{R}}_{e_i}$ is the position vector of *i*th end-effector with respect to the inertial frame (XYZ), respectively. Also, $\vec{\mathbf{r}}_{c_i}$ is the position vector of the adjacent point on the object and *i*th end-effector at the contact point.

The vectorial equation (11) can be written in the following matrix form,

$$\mathbf{R}_{e_i} = \mathbf{R}_o + {}_I\mathbf{C}_o\, \boldsymbol{p}_i, \quad i = 1, \ldots, n. \tag{12}$$

where ${}_I\mathbf{C}_o$ is the rotation matrix of the object frame with respect to the inertial frame and is a function of the object orientation. $\boldsymbol{p}_i$ is the description of $\vec{\mathbf{r}}_{c_i}$ in the object frame, while $\mathbf{R}_{e_i}$ and $\mathbf{R}_o$ are the column vector descriptions of $\vec{\mathbf{R}}_{e_i}$ and $\vec{\mathbf{R}}_o$ in the inertial frame. This vector is a function of $\mathbf{s}_i$. Differentiating Eq. (12) with respect to time, the above constraint equation can be written in the following Pfaffian form

$$\mathbf{A}_{q_i}\dot{\mathbf{q}}_i + \mathbf{A}_{o_i}\dot{\mathbf{q}}_o + \mathbf{A}_{s_i}\dot{\mathbf{s}}_i = \mathbf{0} \quad (i = 1,2, \ldots, n). \tag{13}$$

where

$$\mathbf{A}_{q_i} = \mathbf{J}_i, \quad \mathbf{A}_{o_i} = -\left[\mathbf{I} \quad \frac{\partial {}_I\mathbf{C}_o}{\partial \boldsymbol{\theta}_o}\mathbf{p}_i\right], \quad \mathbf{A}_{s_i} = -{}_I\mathbf{C}_o\left(\frac{\partial \mathbf{p}_i}{\partial \boldsymbol{s}_i}\right), \quad i = 1, \ldots, n, \tag{14}$$

where $\boldsymbol{\theta}_o$ is the vector of the generalized coordinates representing the object orientation and $\mathbf{I}$ is the identity matrix.

https://doi.org/10.1017/S0263574713001069 Published online by Cambridge University Press

Now one can rewrite the motion equations of the whole system as:

$$\begin{aligned}
&\mathbf{M}\ddot{\mathbf{q}} + \mathbf{h} = \mathbf{B}\tau - \mathbf{J}^{\mathrm{T}}\mathbf{F},\\
&\mathbf{M}_{\mathrm{o}}\ddot{\mathbf{q}}_{\mathrm{o}} + \mathbf{h}_{\mathrm{o}} = \mathbf{W}\mathbf{F},\\
&\mathbf{A}_{\mathrm{q}}\ddot{\mathbf{q}} + \mathbf{A}_{\mathrm{o}}\ddot{\mathbf{q}}_{\mathrm{o}} + \mathbf{A}_{\mathrm{s}}\ddot{\mathbf{s}} = \mathbf{b},\\
&\boldsymbol{\alpha}\ddot{\boldsymbol{s}} + \mathbf{D}\mathbf{F} = \mathbf{0},
\end{aligned} \tag{15}$$

where

$$\begin{aligned}
&\mathbf{M} = \mathrm{diag}(\mathbf{M}_1, \ldots, \mathbf{M}_{\mathrm{n}}), \quad \mathbf{J}^{\mathrm{T}} = \mathrm{diag}(\mathbf{J}_1^{\mathrm{T}}, \ldots, \mathbf{J}_{\mathrm{n}}^{\mathrm{T}}), \quad \mathbf{B} = \mathrm{diag}(\mathbf{B}_1, \ldots, \mathbf{B}_{\mathrm{n}}),\\
&\mathbf{A}_{\mathrm{q}} = \mathrm{diag}(\mathbf{A}_{\mathrm{q}_1}, \ldots, \mathbf{A}_{\mathrm{q}_{\mathrm{n}}}), \quad \mathbf{A}_{\mathrm{s}} = \mathrm{diag}(\mathbf{A}_{\mathrm{s}_1}, \ldots, \mathbf{A}_{\mathrm{s}_{\mathrm{n}}}), \quad \boldsymbol{\alpha} = \mathrm{diag}(\boldsymbol{\alpha}_{\mathbf{1}}, \ldots, \boldsymbol{\alpha}_{\mathbf{n}}), \quad \mathbf{D} = \mathrm{diag}(\mathbf{D}_1, \ldots, \mathbf{D}_{\mathrm{n}}),\\
&\mathbf{A}_{\mathrm{o}} = \begin{bmatrix} \mathbf{A}_{\mathrm{o}_1} \\ \vdots \\ \mathbf{A}_{\mathrm{o}_{\mathrm{n}}} \end{bmatrix}, \ \mathbf{h} = \begin{bmatrix} \mathbf{h}_1 \\ \vdots \\ \mathbf{h}_{\mathrm{n}} \end{bmatrix}, \ \mathbf{b} = \begin{bmatrix} \mathbf{b}_1 \\ \vdots \\ \mathbf{b}_{\mathrm{n}} \end{bmatrix}, \mathbf{q} = \begin{bmatrix} \mathbf{q}_1 \\ \vdots \\ \mathbf{q}_{\mathrm{n}} \end{bmatrix}, \ \mathbf{s} = \begin{bmatrix} \mathbf{s}_1 \\ \vdots \\ \mathbf{s}_{\mathrm{n}} \end{bmatrix}, \ \mathbf{F} = \begin{bmatrix} \mathbf{F}_1 \\ \vdots \\ \mathbf{F}_{\mathrm{n}} \end{bmatrix}, \ \tau = \begin{bmatrix} \tau_1 \\ \vdots \\ \tau_{\mathrm{n}} \end{bmatrix},\\
&\text{and} \quad \mathbf{b}_{\mathrm{i}} = -\dot{\mathbf{A}}_{\mathrm{q}_{\mathrm{i}}}\dot{\mathbf{q}}_{\mathrm{i}} - \dot{\mathbf{A}}_{\mathrm{o}_{\mathrm{i}}}\dot{\mathbf{q}}_{\mathrm{o}} - \dot{\mathbf{A}}_{\mathrm{s}_{\mathrm{i}}}\dot{\boldsymbol{s}}_{\mathrm{i}} \quad (\mathrm{i} = 1, 2, \ldots, \mathrm{n}).
\end{aligned} \tag{16}$$

The first equation in Eq. (15) is in fact the assembled equations of motion of all the manipulators. The second equation describes motion of the object. The kinematic constraints resulted from closed kinematic chains are formulated by the third equation. The last equation models the friction and contacts between the end-effectors and the object.

3. Control Synthesis

In order to design the controller, first we convert the constrained equations of motion into a reduced order form and design the controller for the new sets of equations. To avoid any configuration optimization, it is assumed each finger has no redundancy. Considering this assumption, it can be easily shown that $\ddot{\mathbf{q}}$ and $\mathbf{F}$ can be eliminated from Eq. (15) and then it is represented by the following reduced order form,

$$\tilde{\mathbf{M}}\ddot{\mathbf{x}} + \tilde{\mathbf{h}} = \tilde{\mathbf{B}}\tau, \tag{17}$$

where

$$\begin{aligned}
&\tilde{\mathbf{M}} = \begin{bmatrix} \mathbf{M}_{\mathrm{o}} - \mathbf{W}\mathbf{J}^{-\mathrm{T}}\mathbf{M}\mathbf{A}_{\mathrm{q}}^{-1}\mathbf{A}_{\mathrm{o}} & -\mathbf{W}\mathbf{J}^{-\mathrm{T}}\mathbf{M}\mathbf{A}_{\mathrm{q}}^{-1}\mathbf{A}_{\mathrm{s}} \\ \mathbf{D}\mathbf{J}^{-\mathrm{T}}\mathbf{M}\mathbf{A}_{\mathrm{q}}^{-1}\mathbf{A}_{\mathrm{o}} & \boldsymbol{\alpha} + \mathbf{D}\mathbf{J}^{-\mathrm{T}}\mathbf{M}\mathbf{A}_{\mathrm{q}}^{-1}\mathbf{A}_{\mathrm{s}} \end{bmatrix}, \quad \mathbf{x} = \begin{bmatrix} \mathbf{q}_{\mathrm{o}} \\ \mathbf{s} \end{bmatrix},\\
&\tilde{\mathbf{h}} = \begin{bmatrix} \mathbf{h}_{\mathrm{o}} + \mathbf{W}\mathbf{J}^{-\mathrm{T}}\mathbf{M}\mathbf{A}_{\mathrm{q}}^{-1}\mathbf{b} + \mathbf{W}\mathbf{J}^{-\mathrm{T}}\mathbf{h} \\ -\mathbf{D}\mathbf{J}^{-\mathrm{T}}\mathbf{M}\mathbf{A}_{\mathrm{q}}^{-1}\mathbf{b} - \mathbf{D}\mathbf{J}^{-\mathrm{T}}\mathbf{h} \end{bmatrix}, \quad \tilde{\mathbf{B}} = \begin{bmatrix} \mathbf{W} \\ -\mathbf{D} \end{bmatrix}\mathbf{J}^{-\mathrm{T}}\mathbf{B}, \quad \tau = \begin{bmatrix} \tau_1 \\ \vdots \\ \tau_{\mathrm{n}} \end{bmatrix}.
\end{aligned} \tag{18}$$

Considering n cooperating robot arms, each has k_i actuators, and dimensions of the above matrices and vectors are

$$\tilde{\mathbf{M}}\big|_{(n'+n_{\mathrm{o}})\times(n'+n_{\mathrm{o}})}, \quad \mathbf{x}|_{(n'+n_{\mathrm{o}})\times 1}, \quad \tilde{\mathbf{h}}\big|_{(n'+n_{\mathrm{o}})\times 1}, \quad \tilde{\mathbf{B}}\big|_{(n'+n_{\mathrm{o}})\times k}, \quad \tau|_{k\times 1}, \tag{19}$$

where n_o is the number of generalized coordinates of the object, n' is the number of slippage coordinates, and $k = k_1 + \ldots + k_n$ is the number of all actuators in the system. For a planar system with n manipulator $n' = n$, while for spatial one $n' = 2n$.

Equation (17) represents an input–output form of motion equation with k inputs and $n' + n_o$ outputs. Considering size of the vectors and matrices, it can be realized that the system in a planar case can be underactuated only in a cooperating system consisting of two manipulators. Since there are n contact points, Eq. (17) describes a multi-phase dynamic system with $2^{n'}$ phases.

To design a controller based on Eq. (17), one has to consider the internal stability of the system and show that $\tilde{\mathbf{M}}$ is not continuously singular. The internal stability for a general multi-manipulator cooperating system is elaborated in the following theorem. A similar theorem is presented for two-manipulator cooperating system in ref. [25].

https://doi.org/10.1017/S0263574713001069 Published online by Cambridge University Press

Theorem 1. *The system of Fig. 2 represented by Eq. (17) is internally stable if it is input–output stable.*

Proof. Assuming input–output stability means τ, $\mathbf{q}_o$, $\dot{\mathbf{q}}_o$, $\mathbf{s}$, and $\dot{\mathbf{s}}$are bounded. Since the position of the finger tips are continuous and differentiable functions of $\mathbf{q}_o$, $\dot{\mathbf{q}}_o$, $\mathbf{s}$, and $\dot{\mathbf{s}}$, it can be concluded from Eq. (11) that the position of the finger tips and their derivatives are also bounded. Considering this and the fact that $\dot{\mathbf{q}}$ is related to the finger tips velocity and trigonometric functions of $\mathbf{q}$, it results in boundedness of $\dot{\mathbf{q}}$ and consequently $\mathbf{q}$. Using Eqs. (1) and (3), one can show that $\mathbf{F}$ is also bounded.

Theorem 2. $\tilde{\mathbf{M}}$ *is invertible if and only if*

$$\delta_1 \mathbf{I} \leq \int_{t_0}^{t_0+T} \tilde{\mathbf{M}}_d \tilde{\mathbf{M}}_d^T dt \leq \delta_2 \mathbf{I}, \tag{20}$$

for all t_0, where $\tilde{\mathbf{M}}_d = \tilde{\mathbf{M}}(\mathbf{q}_o^{des}, \mathbf{s}^{des})$.$\delta_1$, δ_2, and T are positive constant scalars and $\mathbf{I}$ is proper identity matrix. Also, $\mathbf{q}_o^{des}$ and $\mathbf{s}^{des}$ are the desired values of $\mathbf{q}_o$ and $\mathbf{s}$, respectively.

Proof. Proof is given in ref. [24].

3.1. Adaptive control synthesis

A property of Eq. (17) is that it can be linearly parameterized. It means that the left-hand side of Eq. (17) can be demonstrated as a multiplication of a matrix, which is a given function of $\mathbf{q}_o$, $\dot{\mathbf{s}}$, and their higher-order derivatives and a vector of such parameters as the entire mass, moment of inertia, coefficients of friction, etc. Therefore, one can rewrite the left-hand side of Eq. (17) as

$$\tilde{\mathbf{M}}\ddot{\mathbf{x}} + \tilde{\mathbf{h}} = \mathbf{U}\boldsymbol{\varphi}. \tag{21}$$

In Eq. (21), φ is the unknown parameter column vector and $\mathbf{U}$ is the regression matrix. Assuming φ has the estimated value$\hat{\varphi}$, one can write

$$\hat{\tilde{\mathbf{M}}}\ddot{\mathbf{x}} + \hat{\tilde{\mathbf{h}}} = \mathbf{U}\hat{\boldsymbol{\varphi}}. \tag{22}$$

Theorem 3. *Consider a system expressed by Eq. (17) and assume that the unknown parameter vector* $\boldsymbol{\varphi}$ *does not contribute in* $\tilde{\mathbf{B}}$*, i.e.,* $\hat{\tilde{\mathbf{B}}} = \tilde{\mathbf{B}}$*, with the controller law*

$$\tau = \tilde{\mathbf{B}}^{+}\hat{\tilde{\mathbf{M}}}\left(\ddot{\mathbf{x}}^{des} + \mathbf{K}_v\dot{\mathbf{e}} + \mathbf{K}_p\mathbf{e}\right) + \tilde{\mathbf{B}}^{+}\hat{\tilde{\mathbf{h}}} + (\mathbf{I} - \tilde{\mathbf{B}}^{+}\tilde{\mathbf{B}})\mathbf{y}, \tag{23}$$

and the update rule

$$\dot{\hat{\boldsymbol{\varphi}}} = \Gamma\mathbf{U}^{\mathrm{T}}\hat{\tilde{\mathbf{M}}}^{-\mathrm{T}}\mathbf{E}^{\mathrm{T}}\mathbf{P}\xi. \tag{24}$$

The tracking error goes asymptotically to zero and the parameter estimates remain bounded. In the proposed controller and update rule, $()^+$ is Moore-Penrose generalized inverse of (), $\mathbf{y}$ is an arbitrary vector due to the null space of $\tilde{\mathbf{B}}$, $\mathbf{K}_v$ and Γ are constant diagonal positive definite matrices, $\mathbf{e} = \mathbf{x}^{des} - \mathbf{x}$, $\mathbf{x}^{des} = [\,\mathbf{q}_o^{des^{\mathrm{T}}} \quad \mathbf{0}\,]^{\mathrm{T}}$, $\xi = [\,\mathbf{e}^{\mathrm{T}} \quad \dot{\mathbf{e}}^{\mathrm{T}}\,]^{\mathrm{T}}$, and $\mathbf{E} = [\,\mathbf{0} \quad \mathbf{I}]^{\mathrm{T}}$. Since the system under consideration is a multi-phase system, in contrast to standard methods where $\mathbf{K}_p$ is normally a constant positive definite matrix, here, it is selected to be a constant semi-positive definite matrix. This will be discussed in the Appendix. Also $\mathbf{P}$ is a constant symmetric positive definite solution to the Riccati equation,

$$\mathbf{A}^{\mathrm{T}}\mathbf{P} + \mathbf{P}\mathbf{A} = -\mathbf{Q}, \tag{25}$$

https://doi.org/10.1017/S0263574713001069 Published online by Cambridge University Press

where $\mathbf{Q}$ is a constant positive definite matrix and

$$\mathbf{A} = \begin{bmatrix} \mathbf{0} & \mathbf{I} \\ -\mathbf{K}_p & -\mathbf{K}_v \end{bmatrix}. \tag{26}$$

Proof. Proof of this theorem is almost similar to the Adaptive Computed-Torque Controller given in ref. [26].

Theorem 4. *Consider the system shown in Fig. 2 where its dynamic is described by Eq. (17), with the controller law*

$$\boldsymbol{\tau} = \hat{\tilde{\mathbf{B}}}^{+}\hat{\tilde{\mathbf{M}}}\left(\ddot{\mathbf{x}}^{des} + \mathbf{K}_v\dot{\mathbf{e}} + \mathbf{K}_p\mathbf{e}\right) + \hat{\tilde{\mathbf{B}}}^{+}\hat{\tilde{\mathbf{h}}} + (\mathbf{I} - \hat{\tilde{\mathbf{B}}}^{+}\hat{\tilde{\mathbf{B}}})\mathbf{y}, \tag{27}$$

and the update law

$$\dot{\hat{\boldsymbol{\varphi}}} = \Gamma\mathbf{U}^{\mathrm{T}}\hat{\tilde{\mathbf{M}}}^{-\mathrm{T}}\mathbf{E}^{\mathrm{T}}\mathbf{P}\xi - \sigma_s\hat{\boldsymbol{\varphi}}, \tag{28}$$

where

$$\sigma_s = \begin{cases} 0 & \text{if} \quad \|\hat{\boldsymbol{\varphi}}\| < \varphi_0 \\ \frac{\|\hat{\boldsymbol{\varphi}}\|}{\varphi_0} - 1 & \text{if} \quad \varphi_0 \le \|\hat{\boldsymbol{\varphi}}\| \le 2\varphi_0 \\ 1 & \text{if} \quad \|\hat{\boldsymbol{\varphi}}\| > 2\varphi_0 \end{cases}, \tag{29}$$

The tracking error will be confined to a residual set and all the closed loop signals are bounded. In the proposed controller and update rule, all the definitions are the same as in Theorem 3 except $\mathbf{y}$, which is an arbitrary vector due to the null space of $\hat{\tilde{\mathbf{B}}}$. φ_0 is the upper bound for norm of the uncertain parameters, $\|\boldsymbol{\varphi}\|$.

Proof. Substituting Eq. (27) for Eq. (17), we obtain

$$\tilde{\mathbf{M}}\ddot{\mathbf{x}} + \tilde{\mathbf{h}} = \tilde{\mathbf{B}}\left(\hat{\tilde{\mathbf{B}}}^{+}\hat{\tilde{\mathbf{M}}}\left(\ddot{\mathbf{x}}^{des} + \mathbf{K}_v\dot{\mathbf{e}} + \mathbf{K}_p\mathbf{e}\right) + \hat{\tilde{\mathbf{B}}}^{+}\hat{\tilde{\mathbf{h}}} + (\mathbf{I} - \hat{\tilde{\mathbf{B}}}^{+}\hat{\tilde{\mathbf{B}}})\mathbf{y}\right). \tag{30}$$

Let us rewrite

$$\tilde{\mathbf{B}} = \hat{\tilde{\mathbf{B}}} + \Delta\tilde{\mathbf{B}}. \tag{31}$$

Using Eq. (31), Eq. (30) can be rewritten as

$$\tilde{\mathbf{M}}\ddot{\mathbf{x}} + \tilde{\mathbf{h}} = \hat{\tilde{\mathbf{B}}}\left(\hat{\tilde{\mathbf{B}}}^{+}\hat{\tilde{\mathbf{M}}}\left(\ddot{\mathbf{x}}^{des} + \mathbf{K}_v\dot{\mathbf{e}} + \mathbf{K}_p\mathbf{e}\right) + \hat{\tilde{\mathbf{B}}}^{+}\hat{\tilde{\mathbf{h}}} + (\mathbf{I} - \hat{\tilde{\mathbf{B}}}^{+}\hat{\tilde{\mathbf{B}}})\mathbf{y}\right) + \boldsymbol{\tau}_d, \tag{32}$$

where

$$\boldsymbol{\tau}_d = \Delta\tilde{\mathbf{B}}\left(\hat{\tilde{\mathbf{B}}}^{+}\hat{\tilde{\mathbf{M}}}\left(\ddot{\mathbf{x}}^{des} + \mathbf{K}_v\dot{\mathbf{e}} + \mathbf{K}_p\mathbf{e}\right) + \hat{\tilde{\mathbf{B}}}^{+}\hat{\tilde{\mathbf{h}}} + (\mathbf{I} - \hat{\tilde{\mathbf{B}}}^{+}\hat{\tilde{\mathbf{B}}})\mathbf{y}\right). \tag{33}$$

$\boldsymbol{\tau}_d$ can be named as unmodeled dynamic or disturbances. Note that in the case of bounded errors and parameter estimations, $\boldsymbol{\tau}_d$ will be bounded as well.

Since

$$\hat{\tilde{\mathbf{B}}}(\mathbf{I} - \hat{\tilde{\mathbf{B}}}^{+}\hat{\tilde{\mathbf{B}}}) = \mathbf{0}, \tag{34}$$

https://doi.org/10.1017/S0263574713001069 Published online by Cambridge University Press

Eq. (32) yields

$$\tilde{\mathbf{M}}\ddot{\mathbf{x}} + \tilde{\mathbf{h}} - \mathbf{R}\hat{\tilde{\mathbf{M}}}\left(\ddot{\mathbf{x}}^{des} + \mathbf{K}_v\dot{\mathbf{e}} + \mathbf{K}_p\mathbf{e}\right) - \mathbf{R}\hat{\tilde{\mathbf{h}}} - \boldsymbol{\tau}_d = \mathbf{0}, \tag{35}$$

where $\mathbf{R} = \hat{\tilde{\mathbf{B}}}\hat{\tilde{\mathbf{B}}}^{+}$.

Performing some matrix operations and using Eqs. (21) and (22), one can rewrite Eq. (35) as

$$(\mathbf{I} - \mathbf{R})\,\mathbf{U}\boldsymbol{\varphi} = \mathbf{R}\hat{\tilde{\mathbf{M}}}\mathbf{L}(\mathbf{e}) - \mathbf{R}\mathbf{U}\tilde{\boldsymbol{\varphi}} + \boldsymbol{\tau}_d, \tag{36}$$

where

$$\mathbf{L}(\mathbf{e}) = \ddot{\mathbf{e}} + \mathbf{K}_v\dot{\mathbf{e}} + \mathbf{K}_p\mathbf{e}. \tag{37}$$

and $\tilde{\boldsymbol{\varphi}} = \boldsymbol{\varphi} - \hat{\boldsymbol{\varphi}}$. Using Eqs. (21), (27), and (32), we obtain

$$\mathbf{U}\boldsymbol{\varphi} = \hat{\tilde{\mathbf{B}}}\boldsymbol{\tau} + \boldsymbol{\tau}_d, \tag{38}$$

Substituting the above equation for Eq. (36) yields

$$\mathbf{R}\left(\hat{\tilde{\mathbf{M}}}\mathbf{L}(\mathbf{e}) - \mathbf{U}\tilde{\boldsymbol{\varphi}} + \boldsymbol{\tau}_d\right) = \mathbf{0}. \tag{39}$$

By proper selection of $\mathbf{K}_p$, this equation always results in

$$\hat{\tilde{\mathbf{M}}}\mathbf{L}(\mathbf{e}) - \mathbf{U}\tilde{\boldsymbol{\varphi}} + \boldsymbol{\tau}_d = \mathbf{0}. \tag{40}$$

The reason is discussed in the Appendix.
Choosing the followings states

$$\xi_1 = \mathbf{e},\ \xi_2 = \dot{\mathbf{e}}, \tag{41}$$

Eq. (40) can be represented in the following state space form:

$$\dot{\xi} = \mathbf{A}\xi + \mathbf{E}\mathbf{u}, \tag{42}$$

where

$$\mathbf{u} = \hat{\tilde{\mathbf{M}}}^{-1}\left(\mathbf{U}\tilde{\boldsymbol{\varphi}} - \boldsymbol{\tau}_d\right), \tag{43}$$

Now let us define the following positive definite Lyapunov function candidate

$$V(\xi, t) = \xi^{\mathrm{T}}\mathbf{P}\xi + \tilde{\boldsymbol{\varphi}}^{\mathrm{T}}\boldsymbol{\Gamma}^{-1}\tilde{\boldsymbol{\varphi}}. \tag{44}$$

Differentiating V with respect to time yields

$$\dot{V} = \dot{\xi}^{\mathrm{T}}\mathbf{P}\xi + \xi^{\mathrm{T}}\mathbf{P}\dot{\xi} + 2\tilde{\boldsymbol{\varphi}}^{\mathrm{T}}\boldsymbol{\Gamma}^{-1}\dot{\tilde{\boldsymbol{\varphi}}}. \tag{45}$$

Substituting $\dot{\xi}$ from Eq. (42) into Eq. (45) and defining

$$\mathbf{r} = \hat{\tilde{\mathbf{M}}}^{-\mathrm{T}}\mathbf{E}^{\mathrm{T}}\mathbf{P}\xi, \tag{46}$$

$\dot{V}$ is rewritten as

$$\dot{V} = \xi^{\mathrm{T}}\left(\mathbf{P}\mathbf{A} + \mathbf{A}^{\mathrm{T}}\mathbf{P}\right)\xi + 2\tilde{\boldsymbol{\varphi}}^{\mathrm{T}}\mathbf{U}^{\mathrm{T}}\mathbf{r} - 2\boldsymbol{\tau}_d^{\mathrm{T}}\mathbf{r} + 2\tilde{\boldsymbol{\varphi}}^{\mathrm{T}}\boldsymbol{\Gamma}^{-1}\dot{\tilde{\boldsymbol{\varphi}}}, \tag{47}$$

https://doi.org/10.1017/S0263574713001069 Published online by Cambridge University Press

Since $\boldsymbol{\varphi}$ is a constant vector,

$$\dot{\tilde{\boldsymbol{\varphi}}} = -\dot{\hat{\boldsymbol{\varphi}}}. \tag{48}$$

Using Eqs. (25) and (28), it can be seen that

$$\dot{V}(\xi, t) = -\xi^{\mathrm{T}}\mathbf{Q}\xi - 2\sigma_s\tilde{\boldsymbol{\varphi}}^{\mathrm{T}}\boldsymbol{\Gamma}^{-1}\tilde{\boldsymbol{\varphi}} - 2\boldsymbol{\tau}_d^{\mathrm{T}}\mathbf{r} + 2\sigma_s\tilde{\boldsymbol{\varphi}}^{\mathrm{T}}\boldsymbol{\Gamma}^{-1}\boldsymbol{\varphi}. \tag{49}$$

Defining

$$\mathbf{r}_1 = \begin{bmatrix} \xi \\ \tilde{\boldsymbol{\varphi}} \end{bmatrix}, \tag{50}$$

and

$$\boldsymbol{\tau}_d^* = \begin{bmatrix} -2\mathbf{PE}\hat{\hat{\mathbf{M}}}^{-1}\boldsymbol{\tau}_d \\ 2\sigma_s\Gamma^{-1}\boldsymbol{\varphi} \end{bmatrix}, \tag{51}$$

Eq. (49) is rewritten as

$$\dot{V} = -\mathbf{r}_1^{\mathrm{T}}\mathbf{K}^*\mathbf{r}_1 + \mathbf{r}_1^{\mathrm{T}}\boldsymbol{\tau}_d^*, \tag{52}$$

where

$$\mathbf{K}^* = \begin{bmatrix} \mathbf{Q} & \mathbf{0} \\ \mathbf{0} & 2\sigma_s\boldsymbol{\Gamma}^{-1} \end{bmatrix}. \tag{53}$$

Using Rayleigh-Ritz Theorem,[26] one can write Eq. (52) as

$$\dot{V} \leq -\lambda_{\min}\left\{\mathbf{K}^*\right\}\|\mathbf{r}_1\|^2 + \|\mathbf{r}_1\|\left\|\boldsymbol{\tau}_d^*\right\|. \tag{54}$$

From Eq. (54), it is concluded that $\dot{V}$ will be negative if

$$\|\mathbf{r}_1\| > \frac{\mathrm{T}_d^*}{\lambda_{\min}\{\mathbf{K}^*\}}, \tag{55}$$

where $\mathrm{T}_{\mathrm{d}}^*$ is an upper bound for $\|\boldsymbol{\tau}_d^*\|$.

Now we will consider the different cases for $\|\hat{\boldsymbol{\varphi}}\|$:

First case $\|\hat{\boldsymbol{\varphi}}\| > 2\varphi_0$**:** This means parameter estimates become large and $\sigma_s = 1$. Under this condition, $\mathbf{K}^*$ becomes constant and consequently the right-hand side of Eq. (55) becomes constant. Therefore, for $\mathbf{r}_1$, which satisfies Eq. (55), $\dot{V}$ is negative. This means V decreases. If V decreases, then with the definition of the Lyapanov function

$$V(\xi, t) = \mathbf{r}_1^{\mathbf{T}}\begin{bmatrix} \mathbf{P} & \mathbf{0} \\ \mathbf{0} & \boldsymbol{\Gamma}^{-1} \end{bmatrix}\mathbf{r}_1, \tag{56}$$

$\mathbf{r}_1$ has also to decrease. Apparently, the system reaches the position that Eq. (55) is no longer valid and

$$\|\mathbf{r}_1\| \leq \frac{\mathbf{T}_d^*}{\lambda_{\min}\{\mathbf{K}^*\}}, \tag{57}$$

then $\dot{V}$ may be positive, which causes $\mathbf{r}_1$ to increase such that Eq. (55) is satisfied again. Hence, $\mathbf{r}_1$ and consequently ξ and $\tilde{\boldsymbol{\varphi}}$ will be bounded.

Second case $\|\hat{\boldsymbol{\varphi}}\| < \varphi_0$**:** In this case $\sigma_s = 0$ and the update rule is the same as for the case where there is no difference between $\tilde{\mathbf{B}}$ and $\hat{\tilde{\mathbf{B}}}$. Therefore, according to Theorem 3, ξ and $\tilde{\boldsymbol{\varphi}}$ will again be bounded.

https://doi.org/10.1017/S0263574713001069 Published online by Cambridge University Press

Table II. Numerical value for parameters.

$\bar{m}_k$	l_k	$\bar{m}_o$	$\bar{I}_o$	L_o	$\bar{\mu}_1$	$\bar{\mu}_2$
1 (kg)	1 (m)	1 (kg)	0.01042 (kg m^2)	0.1 (m)	0.25	0.25

Table III. Starting values for unknown parameters.

m_1	m_2	m_3	m_4	m_0
1 (kg)	0.6 (kg)	0.9 (kg)	0.6 (kg)	0.5 (kg)

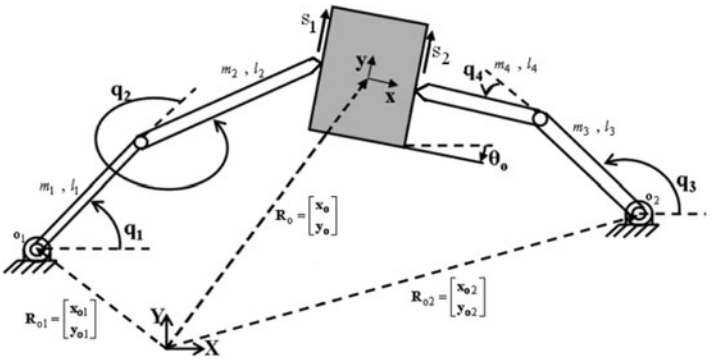

Fig. 4. Schematic of case study.

Third case $\varphi_0 \leq \|\hat{\boldsymbol{\varphi}}\| \leq 2\varphi_0$**:** This is used to ensure that there is a smooth transition between the first and the second cases of update rule and guarantees that no discontinuities will develop.

Note that in the case where the dimension of the null space of $\tilde{\mathbf{B}}$ or $\hat{\tilde{\mathbf{B}}}$ is not zero, $\mathbf{y}$ in Eq. (23) or (27) can have infinite choices. It will let us compute $\boldsymbol{\tau}$ such that the norm of the internal forces becomes minimum.

4. Sample Case

Let us consider a two-fingered hand manipulating a rectangular object. Each finger consists of two rigid links with revolute joints. It is assumed that the object center of mass is located at its geometric center and the whole motion is on the vertical plane. A schematic of the system and object geometry are shown in Fig. 4. Note that since there are two contact points, the system is a four-phase dynamic system, as given below:

- No slippage on either finger tips
- Slippage only on the left finger tip
- Slippage only on the right finger tip
- Slippage on both finger tips

For this system the followings are defined:

$$\mathbf{q}_1 = \begin{bmatrix} q_1 & q_2 \end{bmatrix}^T, \ \mathbf{q}_2 = \begin{bmatrix} q_3 & q_4 \end{bmatrix}^T, \ \mathbf{q}_o = \begin{bmatrix} x_o & y_o & \theta_o \end{bmatrix}^T, \tag{58}$$

Kinematics constraint equations can be written as

$$x_{o1} + l_1 \cos(q_1) + l_2 \cos(q_1 + q_2) + L_o \cos(\theta_o) + s_1 \sin(\theta_o) - x_o = 0,$$
$$y_{o1} + l_1 \sin(q_1) + l_2 \sin(q_1 + q_2) + L_o \sin(\theta_o) - s_1 \cos(\theta_o) - y_o = 0,$$

https://doi.org/10.1017/S0263574713001069 Published online by Cambridge University Press

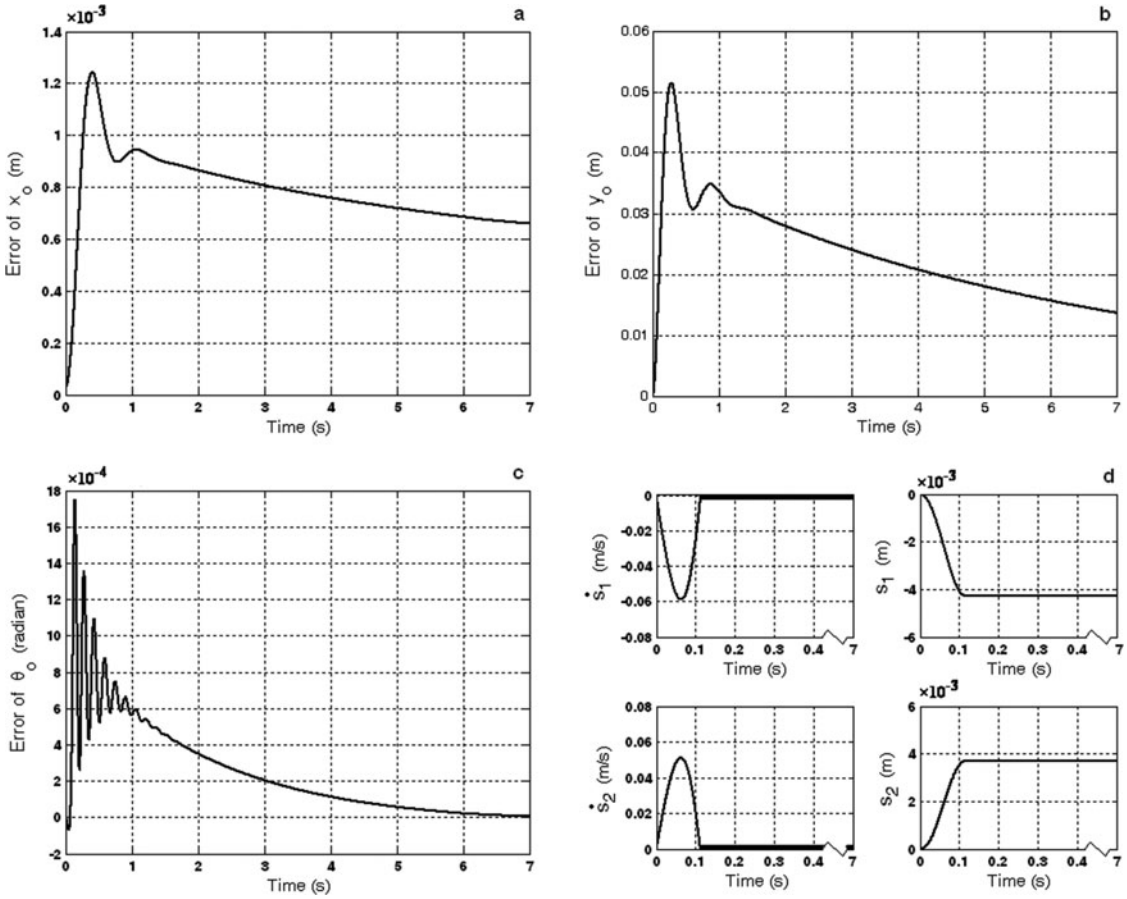

Fig. 5. Trajectory tracking and slippage control performance: (a) object horizontal position error; (b) object vertical position error; (c) object orientation error; (d) left (1) and right (2) finger tip slippages and their velocities.

$$x_{o2} + l_3\cos(q_3) + l_4\cos(q_3+q_4) - \mathrm{L_o}\cos(\theta_\mathrm{o}) + s_2\sin(\theta_\mathrm{o}) - x_\mathrm{o} = 0,$$
$$y_{o1} + l_3\sin(q_3) + l_4\sin(q_3+q_4) - \mathrm{L_o}\sin(\theta_\mathrm{o}) - s_2\cos(\theta_\mathrm{o}) - y_\mathrm{o} = 0, \tag{59}$$

where $\mathrm{L_o}$ is the distance between the object center of mass and its edges (see Fig. 4). The details of matrices and vectors in Eq. (17) for this system are as follows:

$$\tilde{\mathbf{M}} = \begin{bmatrix} \tilde{\mathbf{M}}_{11} & \tilde{\mathbf{M}}_{12} & \tilde{\mathbf{M}}_{13} \\ \tilde{\mathbf{M}}_{21} & \tilde{\mathbf{M}}_{22} & \tilde{\mathbf{M}}_{23} \\ \tilde{\mathbf{M}}_{31} & \tilde{\mathbf{M}}_{32} & \tilde{\mathbf{M}}_{33} \end{bmatrix}, \quad \mathbf{x} = \begin{bmatrix} \mathbf{q}_o \\ s_1 \\ s_2 \end{bmatrix}, \quad \tilde{\mathbf{h}} = \begin{bmatrix} \tilde{\mathbf{h}}_1 \\ \tilde{\mathbf{h}}_2 \\ \tilde{\mathbf{h}}_3 \end{bmatrix}, \quad \tilde{\mathbf{B}} = \begin{bmatrix} \tilde{\mathbf{B}}_{11} & \tilde{\mathbf{B}}_{12} \\ \tilde{\mathbf{B}}_{21} & \tilde{\mathbf{B}}_{22} \\ \tilde{\mathbf{B}}_{31} & \tilde{\mathbf{B}}_{32} \end{bmatrix}, \tag{60}$$

where

$$\tilde{\mathbf{M}}_{11} = \mathbf{M}_\mathrm{o} - \mathbf{W}_1\mathbf{J}_1^{-\mathrm{T}}\mathbf{M}_1\mathbf{A}_{\mathbf{q}_1}^{-1}\mathbf{A}_{\mathrm{o}_1} - \mathbf{W}_2\mathbf{J}_2^{-\mathrm{T}}\mathbf{M}_2\mathbf{A}_{\mathbf{q}_2}^{-1}\mathbf{A}_{\mathrm{o}_2},$$
$$\tilde{\mathbf{M}}_{12} = -\mathbf{W}_1\mathbf{J}_1^{-\mathrm{T}}\mathbf{M}_1\mathbf{A}_{\mathbf{q}_1}^{-1}\mathbf{A}_{\mathrm{s}_1}, \quad \tilde{\mathbf{M}}_{13} = -\mathbf{W}_2\mathbf{J}_2^{-\mathrm{T}}\mathbf{M}_2\mathbf{A}_{\mathbf{q}_2}^{-1}\mathbf{A}_{\mathrm{s}_2},$$
$$\tilde{\mathbf{M}}_{21} = \mathbf{D}_1\mathbf{J}_1^{-\mathrm{T}}\mathbf{M}_1\mathbf{A}_{\mathbf{q}_1}^{-1}\mathbf{A}_{\mathrm{o}_1}, \quad \tilde{\mathbf{M}}_{22} = \mathbf{D}_1\mathbf{J}_1^{-\mathrm{T}}\mathbf{M}_1\mathbf{A}_{\mathbf{q}_1}^{-1}\mathbf{A}_{\mathrm{s}_1} + \alpha_1, \quad \tilde{\mathbf{M}}_{23} = 0,$$
$$\tilde{\mathbf{M}}_{31} = \mathbf{D}_2\mathbf{J}_2^{-\mathrm{T}}\mathbf{M}_2\mathbf{A}_{\mathbf{q}_2}^{-1}\mathbf{A}_{\mathrm{o}_2}, \quad \tilde{\mathbf{M}}_{32} = 0, \quad \tilde{\mathbf{M}}_{33} = \mathbf{D}_2\mathbf{J}_2^{-\mathrm{T}}\mathbf{M}_2\mathbf{A}_{\mathbf{q}_2}^{-1}\mathbf{A}_{\mathrm{s}_2} + \alpha_2,$$
$$\tilde{\mathbf{h}}_1 = \mathbf{h}_\mathrm{o} + \mathbf{W}_1\mathbf{J}_1^{-\mathrm{T}}\mathbf{M}_1\mathbf{A}_{\mathbf{q}_1}^{-1}\mathbf{b}_1 + \mathbf{W}_2\mathbf{J}_2^{-\mathrm{T}}\mathbf{M}_2\mathbf{A}_{\mathbf{q}_2}^{-1}\mathbf{b}_2 + \mathbf{W}_1\mathbf{J}_1^{-\mathrm{T}}\mathbf{h}_1 + \mathbf{W}_2\mathbf{J}_2^{-\mathrm{T}}\mathbf{h}_2,$$

https://doi.org/10.1017/S0263574713001069 Published online by Cambridge University Press

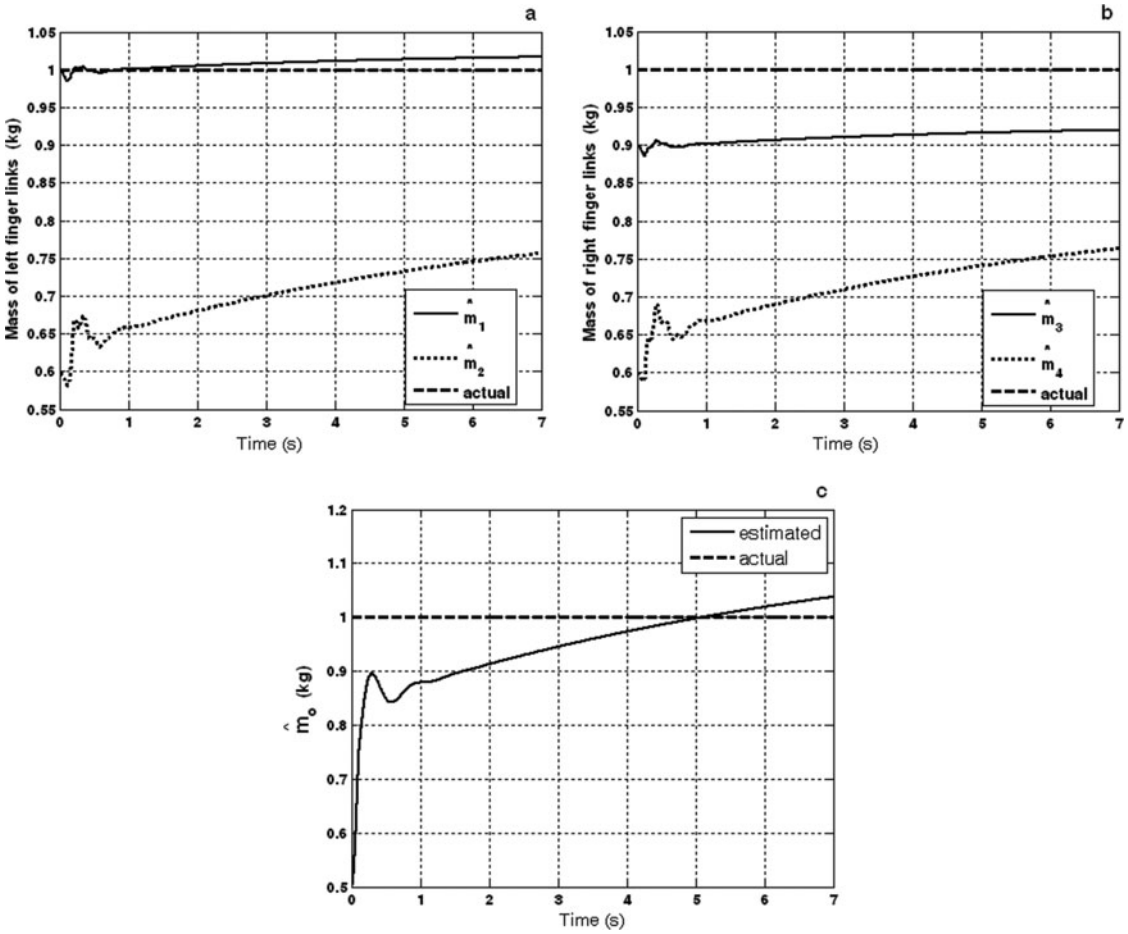

Fig. 6. Performance of parameter estimation: (a) mass of the left finger links; (b) mass of the right finger links; (c) mass of the object.

$$
\begin{aligned}
\tilde{\mathbf{h}}_2 &= -\mathbf{D}_1\mathbf{J}_1^{-\mathrm{T}}\mathbf{h}_1 - \mathbf{D}_1\mathbf{J}_1^{-\mathrm{T}}\mathbf{M}_1\mathbf{A}_{\mathbf{q}_1}^{-1}\mathbf{b}_1,\\
\tilde{\mathbf{h}}_3 &= -\mathbf{D}_2\mathbf{J}_2^{-\mathrm{T}}\mathbf{h}_2 - \mathbf{D}_2\mathbf{J}_2^{-\mathrm{T}}\mathbf{M}_2\mathbf{A}_{\mathbf{q}_2}^{-1}\mathbf{b}_2,\\
\tilde{\mathbf{B}}_{11} &= \mathbf{W}_1\mathbf{J}_1^{-\mathrm{T}}, \qquad \tilde{\mathbf{B}}_{12} = \mathbf{W}_2\mathbf{J}_2^{-\mathrm{T}},\\
\tilde{\mathbf{B}}_{21} &= -\mathbf{D}_1\mathbf{J}_1^{-\mathrm{T}}, \qquad \tilde{\mathbf{B}}_{22} = \begin{bmatrix} 0 & 0 \end{bmatrix},\\
\tilde{\mathbf{B}}_{31} &= \begin{bmatrix} 0 & 0 \end{bmatrix}, \qquad \tilde{\mathbf{B}}_{32} = -\mathbf{D}_2\mathbf{J}_2^{-\mathrm{T}},
\end{aligned} \tag{61}
$$

and

$$
\mathbf{M}_{\mathrm{o}} = \begin{bmatrix} m_{\mathrm{o}} & 0 & 0 \\ 0 & m_{\mathrm{o}} & 0 \\ 0 & 0 & \mathrm{I}_{\mathrm{o}} \end{bmatrix}, \quad \mathbf{h}_{\mathrm{o}} = \begin{bmatrix} 0 \\ m_{\mathrm{o}} g \\ 0 \end{bmatrix}, \quad \mathbf{W}_i = \begin{bmatrix} {}_{\mathrm{I}}\mathbf{C}_{\mathrm{c_i}} \\ [\mathrm{L}_{\mathrm{o}} \quad s_{\mathrm{i}}] \end{bmatrix} \quad (\mathrm{i} = 1, 2), \tag{62}
$$

where

$$
{}_{\mathrm{I}}\mathbf{C}_{\mathrm{c}_1} = \begin{bmatrix} \cos\left(\theta_{\mathrm{o}} + \frac{3\pi}{2}\right) & -\sin\left(\theta_{\mathrm{o}} + \frac{3\pi}{2}\right) \\ \sin\left(\theta_{\mathrm{o}} + \frac{3\pi}{2}\right) & \cos\left(\theta_{\mathrm{o}} + \frac{3\pi}{2}\right) \end{bmatrix}, \quad {}_{\mathrm{I}}\mathbf{C}_{\mathrm{c}_2} = \begin{bmatrix} \cos\left(\theta_{\mathrm{o}} + \frac{\pi}{2}\right) & -\sin\left(\theta_{\mathrm{o}} + \frac{\pi}{2}\right) \\ \sin\left(\theta_{\mathrm{o}} + \frac{\pi}{2}\right) & \cos\left(\theta_{\mathrm{o}} + \frac{\pi}{2}\right) \end{bmatrix}. \tag{63}
$$

Note that all of the above matrices and vectors depend on $\mathbf{q}_1$, $\mathbf{q}_2$, $\mathbf{q}_{\mathrm{o}}$, s_1, s_2 and their derivatives.

In order to verify the performance of the controller discussed and the update rule, the simulation results are presented for the two different cases.

https://doi.org/10.1017/S0263574713001069 Published online by Cambridge University Press

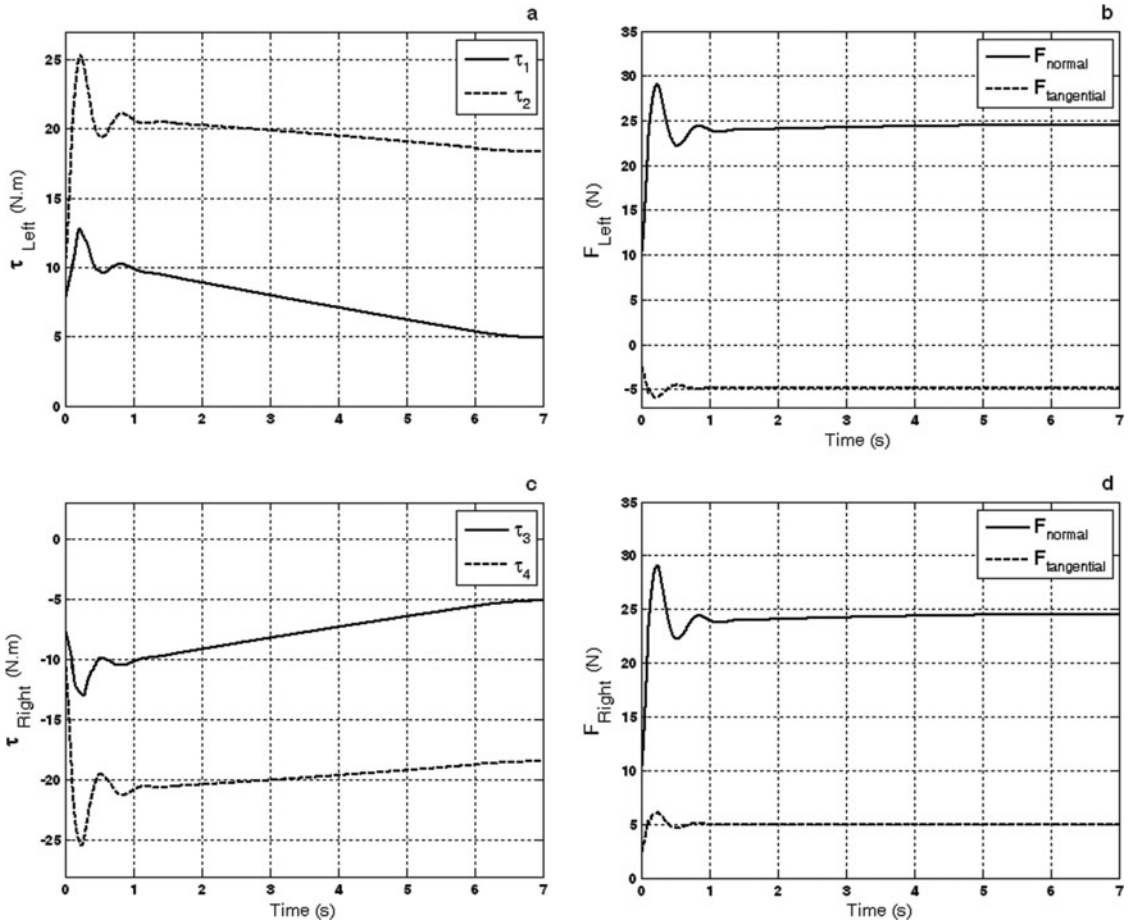

Fig. 7. Time history of: (a) joint torques of the left finger; (b) force exerted to the object by the left finger; (c) joint torques of the right finger; (d) force exerted to the object by the right finger.

Case I: mass of the finger links and the object are assumed to be unknown.

Case II: mass properties of the object as well as friction coefficients between the finger tips and the object surface are assumed to be unknown.

Case II is in fact a more realistic case, because usually we only know geometry of the object.

For both cases the actual properties of the system components are shown in Table II, where $k = 1$, . . ., 4. Also, in both cases, the object is assumed to track the following desired trajectory:

$$\ddot{y}_{\mathrm{o}}^{\mathrm{des}} = \begin{cases} 0.0256 & 0 < t < 1 \\ 0 & 1 \le t < 6 \\ -0.0256 & 6 \le t < 7 \end{cases}, \quad y_{\mathrm{o}}^{\mathrm{des}}(0) = 0.366,\ \dot{y}_{\mathrm{o}}^{\mathrm{des}}(0) = 0, \tag{64}$$

$$x_{\mathrm{o}}^{\mathrm{des}}(t) = 1.466, \quad \theta_{\mathrm{o}}^{\mathrm{des}}(t) = 0.$$

4.1. Case I

In this case, the unknown parameters do not contribute in $\tilde{\mathbf{B}}$. It means, $\tilde{\mathbf{B}} = \hat{\tilde{\mathbf{B}}}$. Therefore, $\boldsymbol{\tau}_d = \mathbf{0}$ and one can use Theorem 3 directly. The non-zero diagonal entries of $\mathbf{K_p}$, $\mathbf{K_v}$, and $\boldsymbol{\Gamma}$ matrices are assumed 100, 10, and 1.28, respectively. The update rule starts with the following values for the estimation procedure (Table III):

https://doi.org/10.1017/S0263574713001069 Published online by Cambridge University Press

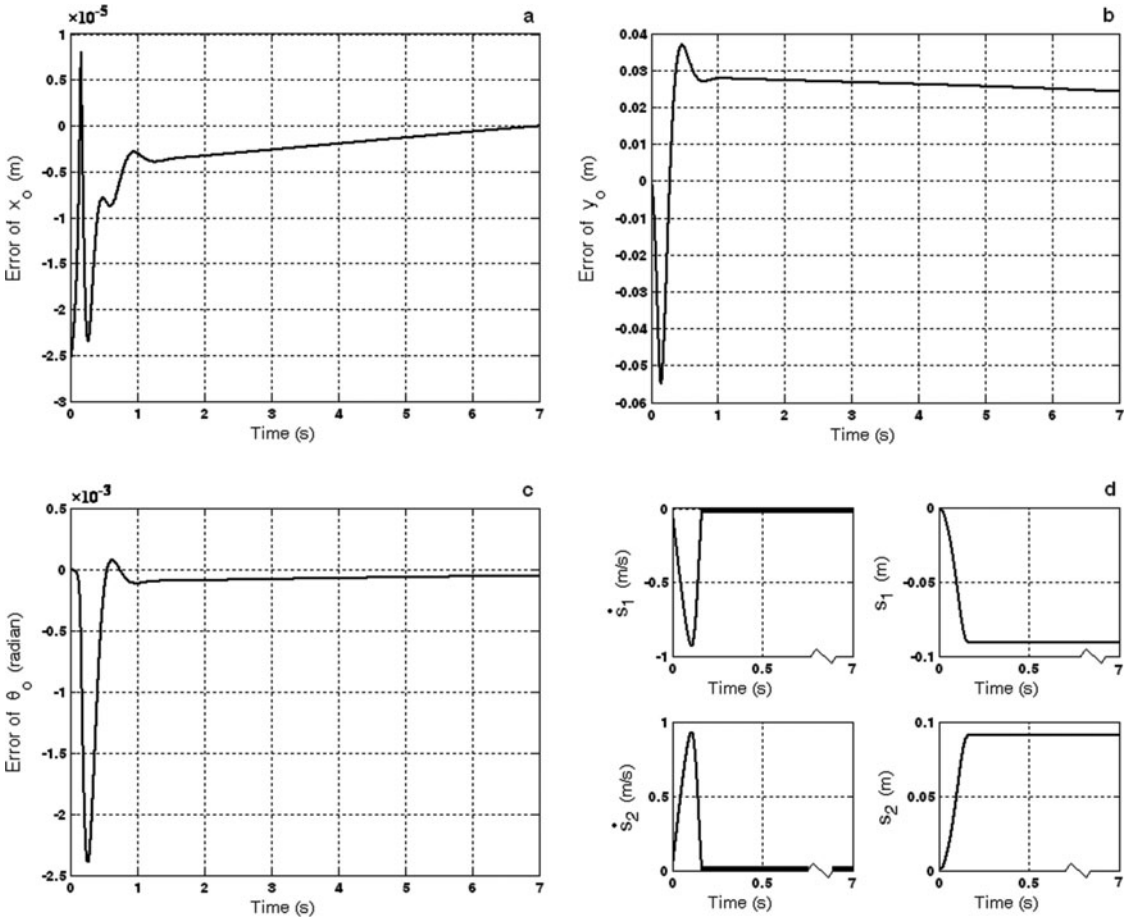

Fig. 8. Trajectory tracking performance: (a) object horizontal position error; (b) object vertical position error; (c) object orientation error; (d) slippage control performance.

Performance of such proposed adaptive control as trajectory tracking, slippage control, and parameter estimations are shown in Fig. 5. Figures 5(a)–(c) show the tracking errors, while Fig. 5(d) shows the left and right finger tip slippages and their velocities. Figure 6 shows the estimated parameters. Actuating torques as well as normal and tangential forces exerted on the object by the left and right fingers are shown in Fig. 7. As can be seen in Figs. 5 and 6, slippage velocities have been controlled and converged to zero, while controller forces the object to track its desired trajectory. At the same time, estimates for unknown parameters remain bounded

Figure 5(d) shows that in the very beginning of the system operation (about 0.1 s), the controller is able to stop the slippages of the fingertips. These slippages are in fact due to the differences between the system parameters used in the controller and their real values. Figure 6 also shows that for this case study, it takes about 1 s that the variation of estimated parameters slows down and they become more stationary. The same trend, rapid variation in the first second and becoming more stationary after, can be seen in the time history of the tracking errors (Figs. 5(a)–(c) and actuating torques and contact forces (Fig. 7)

4.2. Case II

In this case $\tilde{\mathbf{B}} \neq \hat{\tilde{\mathbf{B}}}$. Initial values for friction coefficients and mass properties are assumed to be $\mu_1 = \mu_2 = 1.2$, $m_o = 0.5(\text{kg})$, and $I_o = 0.02(\text{kg.m}^2)$. $\varphi_0 = 1.2\|\boldsymbol{\mu}\|$, where $\boldsymbol{\mu} = [\,\mu_1 \quad \mu_2\,]^{\mathbf{T}}$ and $\| \bullet \|$ is the Euclidian norm. The numerical values for $\mathbf{K_p}$, $\mathbf{K_v}$, and $\boldsymbol{\Gamma}$ are as before.

Performance of the proposed controller is shown in Fig. 8. Like Section 4.1, Figs. 8(a)–(d) show the object tracking errors, the finger tips slippage, and their velocities. While estimated parameters and joints torques and contact forces are shown in Figs. 9 and 10, respectively. It is seen that the

https://doi.org/10.1017/S0263574713001069 Published online by Cambridge University Press

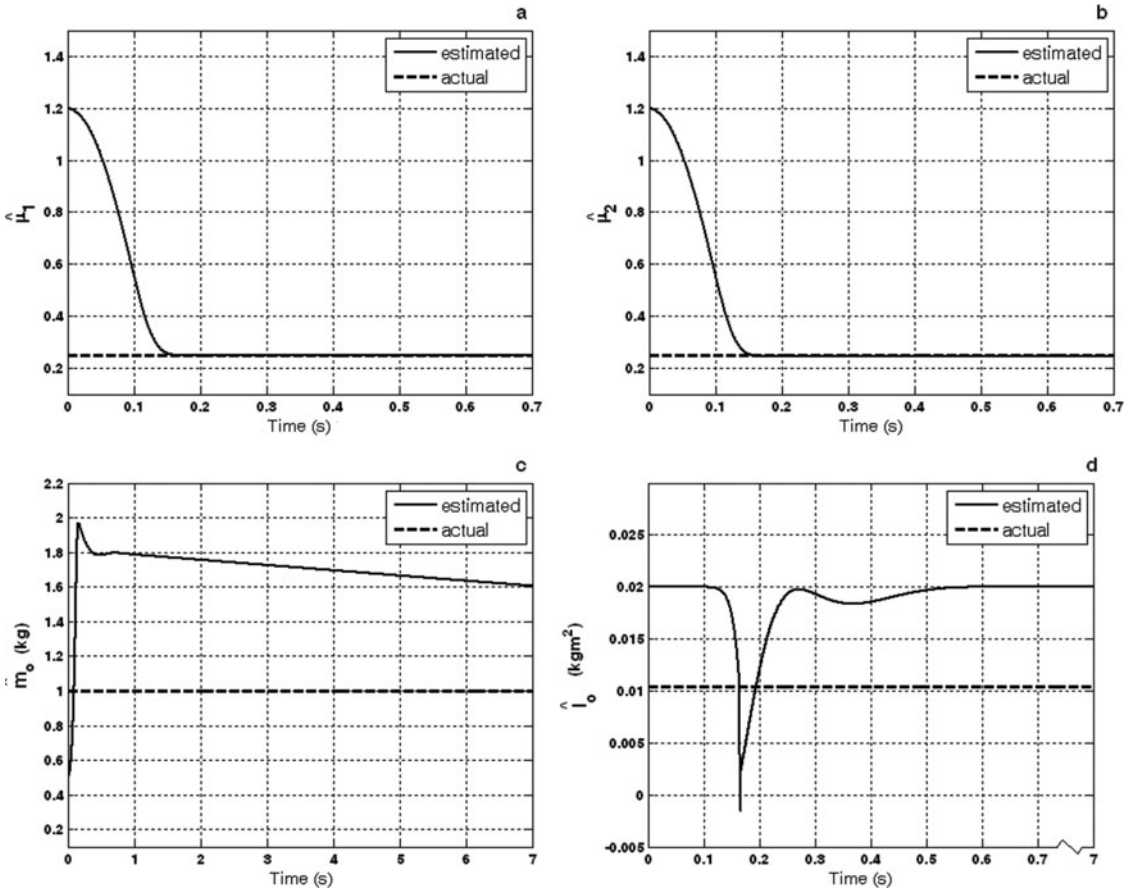

Fig. 9. Performance of parameters estimation: (a) and (b) coefficient of friction between the left and right finger tips and the object surface; (c) the object mass; (d) the object moment of inertia.

controller succeeds in stopping the slippage and reducing the object tracking error while estimation errors remain bounded.

Similar discussion as that presented for the previous case can be presented here for the details of the simulation results in this case.

5. Conclusion

In this paper, the design of an adaptive controller for an *n*-fingered hand manipulating an object was analyzed, considering the slippage between finger tips and the object. Using a new model for frictional contact condition, the constrained equations of motion were transformed to a reduced order input–output dynamic model. Since the finger tips can either slide or remain fixed on the object, it was seen that the system is a multi-phase dynamic system. In this model, equations of motion were described only by second-order differential equations, with switching coefficients. The internal stability of this reduced order form was investigated. As a sample case, a two-fingered hand system is studied in more detail.

An adaptive-control law and an update rule were proposed to control the system. The stability of the closed loop system and boundedness of the errors were proved analytically. The performance of the proposed method was studied numerically, considering the two different cases: a system with unknown masses and another system with unknown object parameters. The simulation results showed a very good performance for the method.

Although the simulation results showed promising performance, there are some considerations in implementation of the method in practical cases that should be taken into account. Measuring the

https://doi.org/10.1017/S0263574713001069 Published online by Cambridge University Press

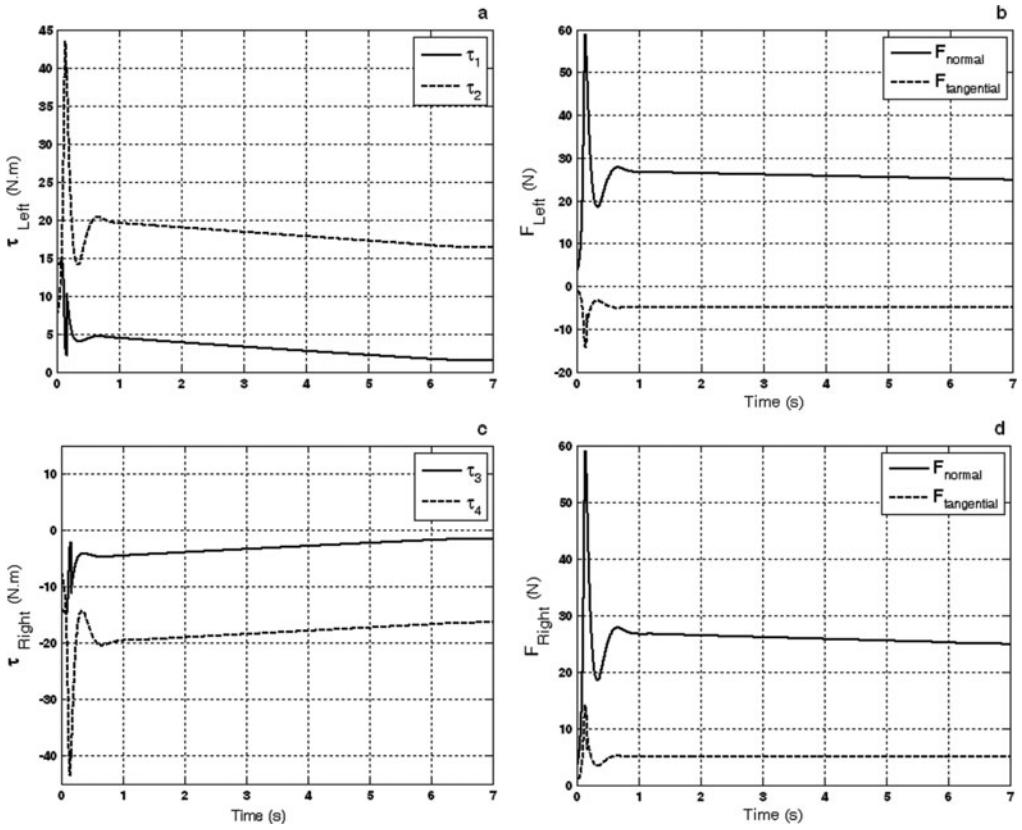

Fig. 10. Time history of: (a) joint torques of the left finger; (b) force exerted to the object by the left finger; (c) joint torques of the right finger; (d) force exerted to the object by the right finger.

required slippage states, complexity in the contact model due to soft finger and distributed contacts, three-dimensional system, and real-time implementation are among these considerations.

Acknowledgements

The authors acknowledge the support and encouragement provided by the Dynamics & Robotics Research Group, Isfahan University of Technology, in the course of the research leading to the compilation of this paper.

References

1. F. Reuleaux, *The Kinematics of Machinery* (Dover, New York, 1963).
2. J. K. Salisbury and B. Roth, "Kinematic and force analysis of articulated mechanical hands," *ASME J. Mech. Transmissions Automat. Des.* **105**(1), 35–41 (1983).
3. B. Mishra, J. T. Schwartz and M. Sharir, "On the existence and synthesis of multifinger positive grips," *Algorithmica* **2**, 541–558 (1987).
4. A. Bicchi, "On the closure properties of robotic grasping," *Int. J. Robot. Res*. **14**(4), 319–334 (1995).
5. B. Bounab, D. Sidobre and A. Zaatri, "Central Axis Approach for Computing n-Finger Force-Closure Grasps," *Proceedings of the IEEE ICRA Conference on Robotics and Automation*, Pasadena, CA, USA (May 19–23, 2008) pp. 1169–1174.
6. H. Kruger and A. F. van der Steppen, "Partial Closure Grasps: Metrics and Computation," *Proceedings of 2011 IEEE International Conference on Robotics and Automation*, Shanghai, China (May 9–13, 2011) pp. 5024–5030.
7. Y. C. Park and G. P. Starr, "Grasping synthesis of polygonal objects using a three-fingered robot hand," *Int. J. Robot. Res.* **11**(3), 163–184 (1992).
8. C. P. Tung and A. C. Kak, "Fast construction of force-closure grasps," *IEEE Trans. Robot. Automat.* **12** (4), 615–626 (1996).
9. J. Cheong, H. Kruger and A. Frank van der Stappen, "Output-sensitive computation of force-closure grasps of a semi-algebraic object", *IEEE Trans. Automat. Sci. Eng*. **8**(3), 495–505 (2011).

10. E. M. Al-Gallaf, "A Learning Rule-Based Robotics Hand Optimal Force Closure," *Proceedings of the 2nd International Conference on Computational Intelligence, Communication Systems and Networks*, Liverpool, UK (Jul. 28–30, 2010) pp. 60–66.
11. Z. Xue, S. Xia, M. Strand, J. M. Zoellner and R. Dillmann, "A Ray-Shooting Based Quality Measurement for Grasping and Manipulation," *Proceedings of the 2011 IEEE International Conference on Robotics and Biomimetics*, Phuket, Thailand (Dec. 7–11, 2011) pp. 1930–1935.
12. R. Krug, D. Dimitrov, K. Charusta and B. Iliev, "On the Efficient Computation of Independent Contact Regions for Force Closure Grasps," *Proceedings of the 2010 IEEE/RSJ International Conference on Intelligent Robots and Systems*, Taipei, Taiwan (Oct. 18–22, 2010) pp. 586–591.
13. R. Platt, Jr., A. H. Fagg and R. A. Grupen, "Null-space grasp control: Theory and experiments," *IEEE Trans. Robot.* **26**(2), 282–295 (2010).
14. X. Y. Zhu and J. Wang, "Synthesis of force-closure grasps on 3-D objects based on the Q distance," *IEEE Trans. Robot. Automat.* **19**(4), 669–679 (2003).
15. R. Platt, Jr., A. H. Fagg and R. A. Grupen, "Nullspace Composition of Control Laws for Grasping," *Proceedings of the IEEE/RSJ International Conference on Intelligent Robots and Systems*, Lausanne, Switzerland (Sep. 30–Oct. 4, 2002) pp. 1717–1723.
16. T. Miyabe, M. Yamamo, A. Konno and M. Uchiyama, "An Approach Toward a Robust Object Recovery with Flexible Manipulators," *Proceedings of the IEEE/RSJ International Conference on Intelligent Robots and Systems*, Maui, HI, USA (Oct. 29–Nov. 3, 2001) pp. 907–912.
17. J. W. Li, H. Liu and H. G. Cai, "On computing three-finger force-closure grasps of 2-D and 3-D objects," *IEEE Trans. Robot. Automat.* **19**(1), 155–161 (2003).
18. Y. H. Liu, M. L. Lam and D. Ding, "A complete and efficient algorithm for searching 3-D form-closure grasps in the discrete domain," *IEEE Trans. Robot.* **20**(5), 805–816 (2004).
19. I. Kao and M. R. Cutkosky, "Comparison of theoretical and experimental force/motion trajectories for dextrous manipulation with sliding," *Int. J. Robot. Res.* **12**(6), 529–534 (1993).
20. N. Y. Chong, D. Choi and Il. H. Suh, "A Generalized Motion Force Planning Strategy for Multi-Fingered Hands Using Both Rolling and Sliding Contacts," *Proceedings of the IEEE/RSJ International Conference on Intelligent Robots and Systems*, Yokohama, Japan (Jul. 26–30, 1993) pp. 113–120.
21. A. A. Cole, P. Hsu and S. S. Sastry, "Dynamic control of sliding by robot hands for regrasping," *IEEE Trans. Robot. Automat.* **8**(1), 42–52 (1992).
22. X. Z. Zheng, R. Nakashima and T. Yoshikawa, "On dynamic control of finger sliding and object motion in manipulation with multi-fingered hands," *IEEE Trans. Robot. Automat.* **16**(5), 469–481 (2000).
23. T. Phoka and A. Sudsang, "Regrasp Planning of Three-Fingered Hand for a Polygonal Object," *Proceedings of the 2010 IEEE International Conference on Robotics and Automation*, Anchorage, Alaska, USA (May 3–7, 2010) pp. 4328–4333.
24. S. Hadian Jazi, M. Keshmiri and F. Sheikholeslam, "Dynamic analysis and control synthesis of grasping and slippage of an object manipulated by a robot," *Adv. Robot.* **22**, 1559–1584 (2008).
25. S. Hadian Jazi, M. Keshmiri, F. Sheikholeslam, M. Ghobadi Shahreza and Mohammad Keshmiri, "Dynamic analysis and control synthesis of undesired slippage of end-effectors in a cooperative grasping," *Adv. Robot.* **26**, 1693–1726 (2012).
26. F. L. Lewis, C. T. Abdallah and D. M. Dawson, *Control of Robot Manipulators* (Macmillan, New York, 1993).

Appendix

For two-dimensional systems, matrix $\mathbf{R} = \hat{\bar{\mathbf{B}}}\hat{\bar{\mathbf{B}}}^{+}$ is an $n+3$ by k matrix, where n is the number of contact points on the object, or, equivalently, the number of fingers in the system and k is the number of actuators. For systems where the number of actuators exceeds $n+3$, systems with three or more fingers, $\mathbf{R}$ is always invertible and therefore Eq. (39) results in Eq. (40).

For systems with two fingers $\mathbf{R}$ is 5×5, while there are four actuators in the system. In this case, $\mathbf{R}$ is always singular.

Let us assume that states corresponding to non-slipping conditions are in the last rows of state vector, i.e., $x = \begin{bmatrix} \mathbf{q}_o \\ \mathbf{s} \end{bmatrix}$. By inspection, one can see that Eq. (39) can be written as

$$\begin{bmatrix} \mathbf{I}_{5-r} & \mathbf{0} \\ \mathbf{0} & \mathbf{0} \end{bmatrix} \left(\begin{bmatrix} \hat{\bar{\mathbf{M}}}_{11} & \hat{\bar{\mathbf{M}}}_{12} \\ \mathbf{0} & \mathbf{I} \end{bmatrix} \begin{bmatrix} \mathbf{L}(\mathbf{e}_1) \\ \mathbf{L}(\mathbf{e}_2) \end{bmatrix} + \begin{bmatrix} \hat{\bar{\mathbf{h}}}_1 \\ \mathbf{0} \end{bmatrix} - \begin{bmatrix} (\mathbf{W}\boldsymbol{\varphi})_1 \\ \mathbf{0} \end{bmatrix} - \begin{bmatrix} \boldsymbol{\tau}_{d_1} \\ \mathbf{0} \end{bmatrix} \right) = \begin{bmatrix} \mathbf{0} \\ \mathbf{0} \end{bmatrix} \tag{A.1}$$

or,

$$\begin{bmatrix} \mathbf{I}_{5-r} & \mathbf{0} \\ \mathbf{0} & \mathbf{0} \end{bmatrix} \begin{bmatrix} \hat{\bar{\mathbf{M}}}_{11}\mathbf{L}(\mathbf{e}_1) + \hat{\bar{\mathbf{M}}}_{12}\mathbf{L}(\mathbf{e}_2) + \hat{\bar{\mathbf{h}}}_1 - (\mathbf{W}\boldsymbol{\varphi})_1 - \boldsymbol{\tau}_{d_1} \\ \mathbf{L}(\mathbf{e}_2) \end{bmatrix} = \begin{bmatrix} \mathbf{0} \\ \mathbf{0} \end{bmatrix}, \tag{A.2}$$

https://doi.org/10.1017/S0263574713001069 Published online by Cambridge University Press

where r is the number of slipping contact points. $\mathbf{e}_1$ corresponds to the object tracking errors and $\mathbf{e}_2$ to non-slipping contacts. Eq. (A.2) leads to

$$\hat{\tilde{\mathbf{M}}}_{11}\mathbf{L}(\mathbf{e}_1) + \hat{\tilde{\mathbf{M}}}_{12}\mathbf{L}(\mathbf{e}_2) + \hat{\tilde{\mathbf{h}}}_1 - (\mathbf{W}\boldsymbol{\varphi})_1 - \boldsymbol{\tau}_{d_1} = \mathbf{0}. \tag{A.3}$$

Since $\ddot{\mathbf{s}}^{des} = \dot{\mathbf{s}}^{des} = \mathbf{s}^{des} = \mathbf{0}$, one can write

$$\mathbf{L}(\mathbf{e}_2) = -\ddot{\mathbf{s}} - \mathbf{K}_{v2}\dot{\mathbf{s}} - \mathbf{K}_{p2}\mathbf{s}. \tag{A.4}$$

Since $\mathbf{s}$ corresponds to non-slipping condition, $\ddot{\mathbf{s}} = \dot{\mathbf{s}} = \mathbf{0}$. Therefore,

$$\mathbf{L}(\mathbf{e}_2) = -\mathbf{K}_{p2}\mathbf{s}. \tag{A.5}$$

Note that $\mathbf{s}$ is in fact the movement of the finger tips on the object from its initial position, and is not generally zero. If one sets $\mathbf{K}_{p2} = \mathbf{0}$, Eq. (A.3) yields

$$\hat{\tilde{\mathbf{M}}}_{11}\mathbf{L}(\mathbf{e}_1) + \hat{\tilde{\mathbf{h}}}_1 - (\mathbf{W}\boldsymbol{\varphi})_1 - \boldsymbol{\tau}_{d_1} = \mathbf{0}, \mathbf{0} = \mathbf{0}. \tag{A.6}$$

Switching between zero and non-zero values for $\mathbf{K}_{ps}$, from one phase to another, results in non-constant $\mathbf{A}$, Eq. (26), and consequently non-constant $\mathbf{P}$ matrix, Eq. (25).

https://doi.org/10.1017/S0263574713001069 Published online by Cambridge University Press